Sensors & Actuators: B. Chemical 283 (2019) 556–562

Contents lists available at ScienceDirect

Sensors and Actuators B: Chemical

journal homepage: www.elsevier.com/locate/snb

Surface N-doped graphene sheets induced high electrocatalytic activity for selective ascorbic acid sensing

Liangliang Huang[a,b], Yuanyuan Cao[a,*], Dongfeng Diao[a,*]

[a] Institute of Nanosurface Science and Engineering (INSE), Guangdong Provincial Key Laboratory of Micro/Nano Optomechatronics Engineering, Shenzhen University, Shenzhen, 518060, China

[b] Key Laboratory of Optoelectronic Devices and Systems of Ministry of Education and Guangdong Province, College of Optoelectronic Engineering, Shenzhen University, Shenzhen, 518060, China

A R T I C L E I N F O

Keywords:
Ascorbic acid
Electrochemical biosensor
N-doped graphene sheets
Carbon film
Electron cyclotron resonance

A B S T R A C T

In this study, the graphene sheets embedded carbon (GSEC) film was modified with surface N-doping for highly selective ascorbic acid (AA) sensing. We found that the N-doped graphene sheets formed in-situ at the carbon film surface and induced high electrocatalytic activity for AA oxidation. Although surface N-doping slightly decreased the I_D/I_G and surface roughness of carbon film, the graphene sheets embedded in amorphous were preserved. With surface N-doping, the charge-transfer resistance was reduced from 22.5 Ω cm^2 to 3.9 Ω cm^2, the oxidation-reduction peak separation decreased to a low value of 65.7 mV in $Fe(CN)_6^{4-/3-}$ redox system, and the standard rate constant was increased from 0.24×10^{-2} to 1.36×10^{-2} cm·s^{-1}. The surface N-doped graphene sheets embedded carbon (SN-GSEC) decreased the oxidation potential of AA from 0.186 V to 0.025 V (vs. Ag/AgCl) and realized selective detecting of AA. The mechanism may be that the surface N-doping induce the adjacent carbon in graphene sheets to obtain a higher partial density of states and more positive compensating charge. This study provides a simple method for preparing high performance electrochemical biosensor.

1. Introduction

Ascorbic acid (AA) is a soluble vitamin and has been used extensively as an antioxidant in food, drink and medicine [1–5]. The major function of AA is to protect cells from toxicity of reactive oxygen species [6]. Abnormal levels of AA can cause many diseases, including nausea, vomiting, diarrhea, kidney stones et al [7]. It is vital to confirm the AA level by simple and fast detecting methods.

Carbon film electrodes have been widely used in electroanalysis because of their wide potential window, low background current and low cost [8], especially the carbon film with nanocrystalline structure [9–12]. This carbon film has special sp^2 and sp^3 mixed bonds structure and exhibits high electrochemical activity, ultra-flat surface and large potential window (4.1 V) [10,12]. The formation of nanocrystalline is the key to the remarkable electrochemical performance. Diao et al [13] further improved the electrochemical activity by forming up-standing graphene sheets in carbon film. The graphene sheets offered fast electron transport path and more reaction active sites [14]. However, these carbon film electrodes were hard to be applied in detecting AA by electrochemical direct oxidation. Because the interfering of dopamine (DA), which coexisted with AA and seriously affected the accuracy detection for AA [15,16]. The AA and DA exhibited a similar oxidation potential in electrochemical detection for most electrode materials [17,18].

A possible way around this is to modify the electrode surface with an effective catalyst, which could significantly decrease the oxidation overpotential of AA. Such as catechol [19] and glutamic acid [20] have being used to modify carbon electrode for catalyzing the oxidation of AA. N-doped graphene [21] is another excellent catalyst for the oxidation of AA, and could realize simultaneous determination of AA, DA and uric acid (UA). But the instability of the adsorbed or attached catalysts on glassy carbon electrode make these methods limited in application. Consequently, the in-situ forming N-doped graphene embedded in carbon film was proposed. This method not only avoids the disadvantage of physical adsorption of catalyst, but also preserves the advantage of low background currents of carbon film. Niwa et al [22] made important contributions in preparing carbon film with N-doped nanocrystalline by electron cyclotron resonance (ECR) under ion irradiation, the N-doped nanocrystalline greatly improved the electrochemical activity of carbon film. But for the N-doped graphene sheets embedded carbon film, there has no related reports until now.

In this article, we tried to in-situ form N-doped graphene sheets in

---

[*] Corresponding authors.
E-mail addresses: caoyy@szu.edu.cn (Y. Cao), dfdiao@szu.edu.cn (D. Diao).

https://doi.org/10.1016/j.snb.2018.12.079
Received 13 October 2018; Received in revised form 12 December 2018; Accepted 15 December 2018

carbon film by surface N-doping for selective ascorbic acid sensing. The nanostructure and morphology of surface N-doped graphene embedded carbon (SN-GSEC) film were characterized with transmission electron microscopy (TEM), atomic force microscopy (AFM), Raman spectra and X-ray photoelectron spectroscopy (XPS). The effects of surface N-doping on the electrochemical activity of carbon film were studied with electrochemical impedance spectroscopy (EIS) and cyclic voltammetry (CV). The selective detecting AA were investigated with differential pulse voltammetry (DPV).

2. Experimental

2.1. Film fabrication

All carbon films were prepared by using ECR plasma sputtering system under electron irradiation. The pure GSEC film with a thickness of 80 nm were firstly deposited on boron-doped silicon wafer (100) substrate under an electron acceleration voltage of + 80 V. Then, the surface N-doping were performed on the GSEC film with a mixture gas of Ar and N_2. The partial pressure of N_2 was 10%. The chamber pressure kept at 4.00×10^{-2} Pa. The electron acceleration voltage was remained at + 80 V. The thickness of surface N-doped layer was about 8 nm. During the film preparation, the microwave power and DC voltage applied to the carbon target were 500 W and −500 V, respectively.

2.2. Film structure characterization

The effects of surface N-doping on the nanostructure of GSEC film were firstly investigated with high-resolution TEM (Titan3 Themis G2). The TEM samples were prepared by slightly scratching the film surface with a diamond pencil and transferring the films onto a copper microgrid. The roughness and surface morphology were measured by using Dimension Edge AFM with a BRUKER SCANASYS-AIR tip at a scanning rate of 1 Hz with 512 × 512 pixels. Raman spectra were collected on a Raman spectrometer using a 633 nm laser as the excitation source (HORIBA, LabRAM HR Evolution). XPS (ThermoScientific ESCALAB 250Xi) were recorded to investigate the influence of surface N-doping on the elemental composition and the quantity of chemical bonds of GSEC film. The element contents were calculated based on peak area and peak height sensitivity method [23] with Avandage software. The N 1 s spectra were fitted based on the binding energy (BE) values of three chemical bonding states [24] with XPSPeak software.

2.3. Electrochemical characterization

Electrochemical measurements were performed in a standard three-electrode cell by using an electrochemistry workstation of Gamry Reference 600 + . The working electrode was carbon film with an area of o.2 cm^2, the counter and reference electrodes were a Pt wire and Ag/AgCl, respectively. The EIS were measured in 5 mM $Fe(CN)_6^{4-/3-}$ and 0.1 M KCl with a AC signal amplitude of 10 mV in the frequency range of 0.1 Hz to 100 kHz. The DC was set at 0.26 V vs.Ag/AgCl. The CV were measured in 1 mM $Fe(CN)_6^{4-/3-}$ and 1 M KCl. The DPVs of AA, DA and UA in 0.1 M phosphate buffer (PB) solution (pH = 7.0) were carried out with a step size of 5 mV and a pulse size of 25 mV.

3. Results and discussion

3.1. Surface structure and chemical composition

The nanostructures of GSEC and SN-GSEC films were examined with high-resolution TEM. As shown in Fig. 1, the multilayer graphene sheets embedded in the amorphous carbon were formed in both two carbon films. The fast Fourier transformation (FFT) were performed on the red and green squares marked regions. In the red square regions, two white light spots appeared in the FFT images, which confirmed the formation of multilayer graphene. However, in green square regions, FFT showed no pattern corresponding to amorphous structure. The nanostructure of SN-GSEC film is almost the same as GSEC. It indicates that the graphene nanocrystalline structure is remained after being surface N-doped, and the N-doped graphene sheets may be formed on the surface of SN-GSEC film. The film surface were characterized with AFM as shown in Fig. 1. It shows that the roughness of GSEC film is slightly reduced after being surface N-doped. This further confirms that the surface N-doping has no obvious influence on the graphene nanocrystalline structure of GSEC film.

To further characterize the influence of surface N-doping, Raman spectra were examined as shown in Fig. 2. The two spectra are very similar, both of them exhibit clear D, G and 2D peak at about 1345 cm^{-1}, 1595 cm^{-1} and 2756 cm^{-1}, respectively. But the surface N-doping leads to the decreasing of peak intensity ratio of I_D/I_G from 1.33 to 1.03. The I_D/I_G ratio is related to the clustering and ordering of sp^2 phase in stage 2 of Ferrari’s model [25]. It indicates that the clustering and ordering degree of sp^2 phase in the surface N-doped layer is lower than that in GSEC. The 2D band is the most prominent feature of graphene and its shape is sensitive to the number of layers of graphene [26,27]. The appearance of 2D band demonstrates the formation of multilayer graphene sheets in both two films. Therefore, it can be concluded that the graphene sheets are formed in the surface of SN-GSEC film although surface N-doping inhibits the clustering of sp^2 phase at some extent.

To confirm the effects of surface N-doping on the chemical composition and bonding structure, the XPS were examined as shown in Fig. 3 and Table 1. The sp^2 phase content is lower in SN-GSEC than GSEC films, which is consistent with the results of Raman. It indicates that the N-doping inhibits the clustering of sp^2 phase, and results in the decreasing of surface roughness of SN-GSEC slightly. As shown in Fig. 3(b), the N 1 s spectrum of SN-GSEC could be well-fitted into three peaks at the binding energies of 398.4 eV, 399.9 eV and 401.2 eV, corresponding to the pyridinic N, pyrrolic N and graphitic N as depicted in Fig. 3(c), respectively. The nitrogen atoms are mainly bonded with carbon atoms by pyridinic N and graphitic N, both of them are helpful to improve the electrochemical properties of carbon materials [22,28]. The pyridinic N could only exist at the edge regions of six-membered rings [29], which may be the reason that induces the decreasing of I_D/I_G as well as sp^2 phase content. It can be concluded that the N-doped graphene sheets are formed at the surface of SN-GSEC film.

3.2. Electrochemical properties

3.2.1. EIS

EIS is an excellent method for investigating the interface features of modified electrodes [30]. In the present study, the EIS was measured in $Fe(CN)_6^{4-/3-}$ redox system and fitted with Gamry Echem Analyst software based on the Randles equivalent circuit [31] as shown in Fig. 4. The R_s, CPE and W represented the solution resistance, Constant Phase Element and Warburg impedance, respectively. As shown in Table 2, the double-layer capacitance (C_{dl}) of SN-GSEC film was much larger than GSEC. It means the surface N-doping leads to the increasing of double-layer capacitance. The charge-transfer resistance (R_{ct}) are significantly decreased after being surface N-doped. It indicates that the electrode kinetics is extremely sensitive to the surface doping nitrogen. In addition, the standard rate constant (K°) was calculated based on the charge transfer resistance [32], it increased from 0.24×10^{-2} to 1.36×10^{-2} $cm{\cdot}s^{-1}$. This proves the surface N-doping significantly increases electron transfer rate of GSEC film.

3.2.2. CV

The CVs were also measured in $Fe(CN)_6^{4-/3-}$ redox system as shown in Fig. S1(a). The surface N-doping induced that the peak separation (△Ep) decreased from 69.9 mV to 65.7 mV. It should be noted that the 65.7 mV is a very low value and much lower than many other

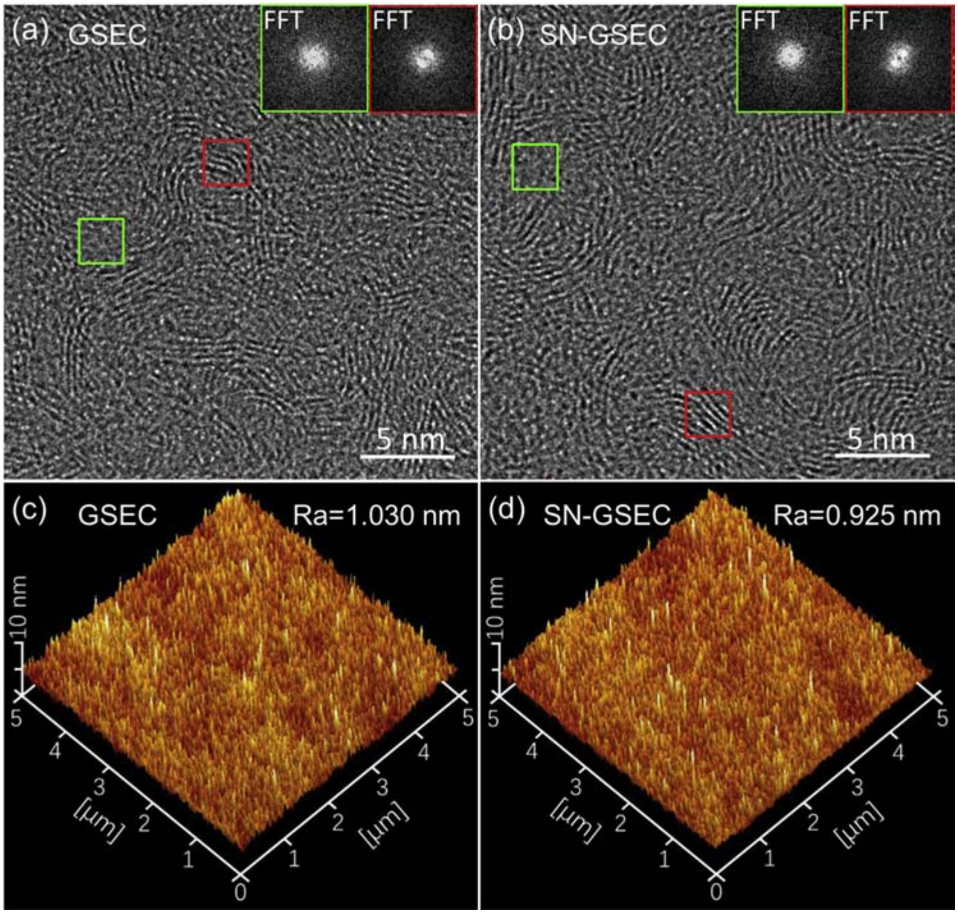

Fig. 1. The TEM and AFM images of GSEC (a)(c) and SN-GSEC (b)(d) films. The FFT images corresponding to green (amorphous) and red (multilayer graphene sheets) squares regions, respectively. (For interpretation of the references to colour in this figure legend, the reader is referred to the web version of this article).

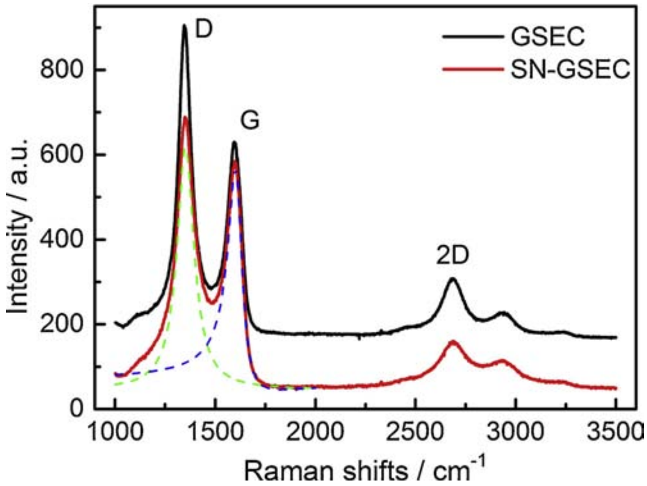

Fig. 2. The Raman spectra of GSEC and SN-GSEC films.

carbon electrodes at same conditions, such as N-doped tetrahedral amorphous carbon [33,34], N-doped carbon nanofibers [35] graphene [36], carbon nanowalls [37] and so on. This indicates that the surface N-doping obviously improves the electrochemical activity of GSEC film. The SN-GSEC film electrode also shows higher oxidation peak current than GSEC film. This may be resulted from that surface N-doping increases the electroactive surface area. As showed in Fig. S2, the CVs with different scanning rate were measured. The electroactive surface area were estimated according to the Randles-Sevcik equation [38] as shown in Fig. S1(b). The surface N-doping results in the increasing of effective active area from 0.175 cm^2 to 0.201 cm^2.

3.2.3. DPV

The DPVs of two carbon film electrodes in 100 μM AA and 0.1 M PB solution were presented in Fig. 5(a). The SN-GSEC film showed much lower oxidation potential and higher current density than GSEC film. Under the interfering of DA and UA, the DPV for AA were also measured as shown in Fig. 5(b). For the GSEC film electrode, three biomolecules only present two oxidation peaks at 0.186 V and 0.306 V. This is because that the oxidation peak of AA overlaps with DA (the oxidation potential of DA at GSEC was 0.21 V as shown in Fig. S3). For the SN-GSEC film electrode, three clearly separated peaks with higher peak currents are appeared at 0.025 V, 0.165 V and 0.295 V, which corresponding to the oxidation of AA, DA and UA, respectively. These results indicate that the overpotential of AA oxidation is remarkably decreased by surface N-doping. The SN-GSEC film has excellent electrocatalytic activity for AA oxidation and could be used to selective detecting AA.

3.3. Mechanism analysis

It's well known that material properties are closely related with its structures, the high electrocatalytic activity of SN-GSEC film for AA oxidation must be resulted from the surface N-doping. Based on the former structural characterization, the nanostructures of SN-GSEC film were depicted in Fig. 6(a). At the under layer, multilayer graphene sheets were formed and embedded in the amorphous carbon. At the surface layer, the N-doped graphene sheets were formed. The nitrogen

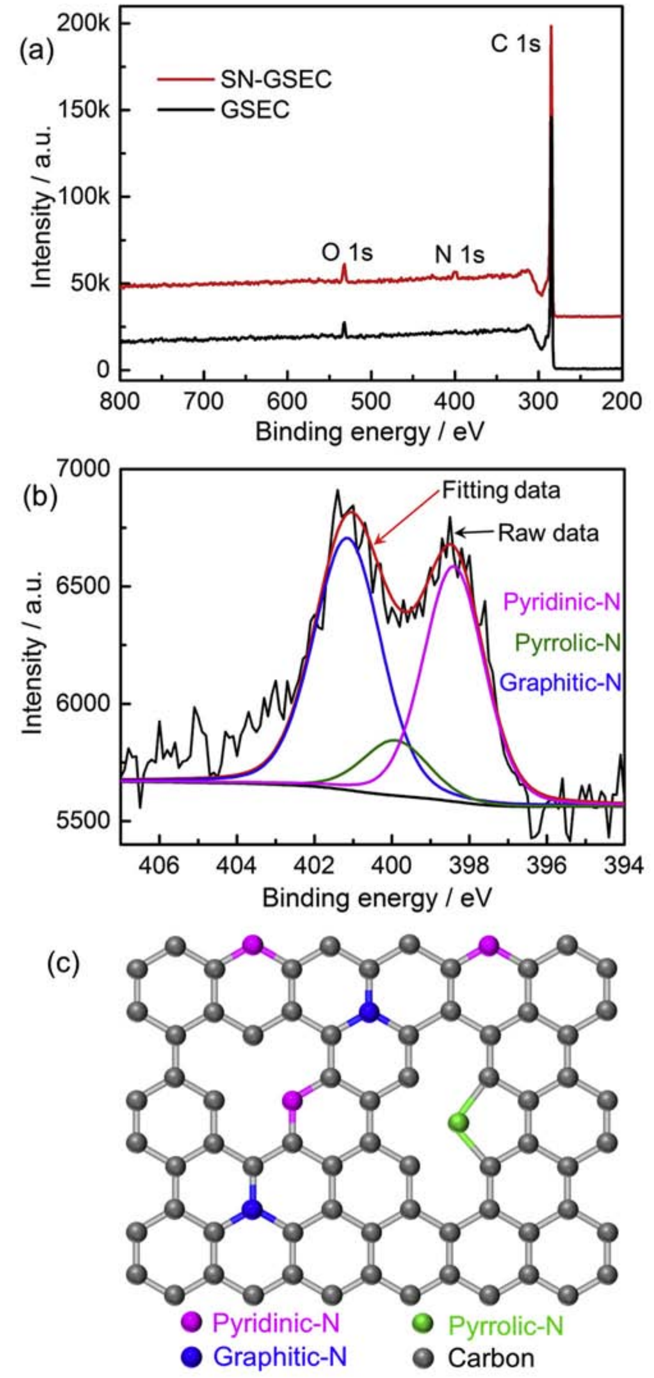

Fig. 3. (a) XPS spectra of GSEC and SN-GSEC films; (b) XPS N 1 s spectrum of SN-GSEC film; (c) Schematic representation of the N-doped graphene.

Table 1
The surface characterization data of carbon films with Raman and XPS.

	I_D/I_G	sp^2 / (sp^2 + sp^3) %	O/C (at. %)	N (at.%)	N 1 s (at%)		
					Pyridinic-N	Pyrrolic-N	Graphitic-N
GSEC	1.33	84.34	3.22	–	–	–	–
SN-GSEC	1.03	80.24	3.12	3.88	40.96	10.41	48.63

atoms were mainly bonded with carbon atoms by pyridinic N and graphitic N. In graphene, N-doping could increase the electronic partial density of states (PDOS) near the Fermi level, especially the adjacent carbon atoms [39]. Higher DOS is helpful to facilitate the electron transfer and increase the electrochemical activity. Consequently, the SN-GSEC exhibited lower charge-transfer resistance and △Ep than GSEC film. Meanwhile, the nitrogen has one more electron than carbon and bears a negative charge of 0.81 e [39–41]. The incorporation of nitrogen atom into graphene will result in redistribution of charge, and the carbon adjacent to nitrogen will get a much larger compensating positive charge than other carbon atoms [40,42,43]. AA is negatively charged at neutral pH [44,45], the positively charged carbon is more likely to attract negatively charged AA, and so, the electron can be more easily transferred from AA to SN-GSEC film via hydrogen bonds [21,46]. Thus, the hydroxyl group is oxidized to carbonyl groups in furan ring as shown in Fig. 6(b). Therefore, the surface N-doping induces the adjacent carbon in graphene sheets to obtain a higher PDOS and more positive compensating charge, which are the main reasons for the excellent electrocatalytic activity and larger electroactive surface area of SN-GSEC.

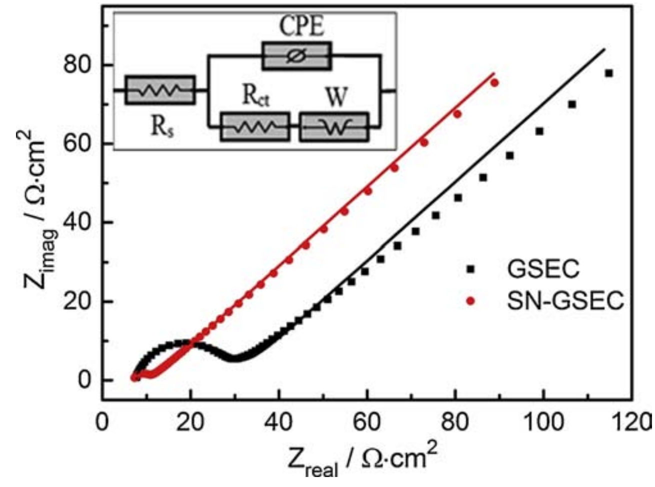

Fig. 4. The Nyquist plots of GSEC and SN-GSEC film electrodes obtained from EIS measurements with 5 mM $Fe(CN)_6^{4-/3-}$ in 0.1 M KCl (The insert is equivalent circuit).

Table 2
The fitted results of EIS measurements.

	R_s / Ω·cm²	C_{dl} / μF·cm^{-2}	n	W_d/ 10^{-3}·Ω^{-1}·s$^{1/2}$	R_{ct} / Ω·cm²	k° / 10^{-2}cm·s^{-1}
GSEC	7.50	16.13	0.859	9.14	22.5	0.24
SN-GSEC	7.18	33.01	0.790	9.08	3.91	1.36

3.4. Electrochemical determination of AA

To assess the detection performance of SN-GSEC film for AA, the DPVs were measured in single AA and mixture of AA, DA and UA in 0.1 M PB solution, respectively. As shown in Figs. 7 and 8 , the DPV signals of AA increased with the AA concentration, and the oxidation current peak intensity versus concentration of AA displayed two different linear response in low concentration and high concentration ranges. The DA and UA also exhibited two different linear response. This phenomenon could be originate from the formation of a monolayer of adsorbed biomolecules at the electrode surface in low concentration ranges [47,48]. In solution of single AA, the detection linear range is from 1 μM to 3 mM with a detection limit of 0.75 μM. In the mixture solution, the detection linear ranges of AA, DA and UA are 3 μM to 1600 μM, 0.75 μM to 400 μM and 0.75 μM to 400 μM with detection limit of 1 μM, 0.25 μM and 0.25 μM as S/N = 3, respectively. It shows the SN-GSEC film possesses better detection sensitivity than some graphene and N-doped graphene [21,49] electrodes. This may be related

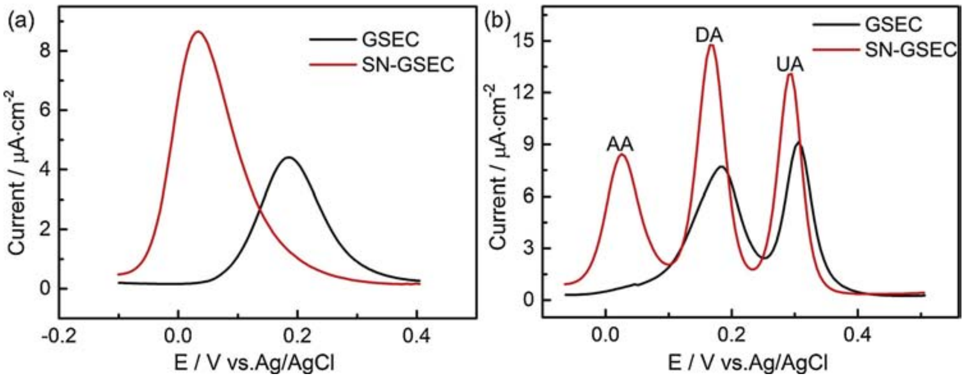

Fig. 5. (a) The DPVs for 100 μM AA in 0.1 M PB solution (pH = 7.0) at GSEC and SN-GSEC film electrodes; (b) The DPVs for 100 μM AA, 25 μM DA and 25 μM UA in 0.1 M PB solution (pH = 7.0) at GSEC and SN-GSEC film electrodes.

with the low surface roughness of SN-GSEC, which result in a background current. In addition, these results not only indicates the SN-GSEC have excellent selective sensing for AA, but also could be used to simultaneous detection of AA, DA and UA.

4. Conclusion

In this study, the SN-GSEC films were prepared for selective AA sensing by ECR plasma sputtering under low-energy electron irradiation condition. We found that the in-situ formed N-doped graphene sheets at the film surface induced high electrocatalytic activity for AA oxidation. Compared with GSEC, the SN-GSEC film decreased the charge-transfer resistance from 22.5 Ω·cm^2 to 3.9 Ω·cm^2, the standard rate constant was increased from 0.24×10^{-2} to 1.36×10^{-2} cm·s^{-1}, and the oxidation-reduction peak separation was decreased to a low value of 65.7 mV in $Fe(CN)_6^{4-/3-}$ redox system. The oxidation potential of AA on GSEC film was decreased from 0.186 V to 0.025 V (vs. Ag/AgCl) by surface N-doping. The SN-GSEC film realized selective detecting AA from 1 μM to 3 mM with a detection limit of 0.75 μM. Furthermore, the SN-GSEC film could be used to simultaneous determination of AA, DA and UA without additional functionalization. The linear detection range for AA, DA and UA are 3 μM to 1600 μM, 0.75 μM to 400 μM and 0.75 μM to 400 μM with detection limit of 1 μM, 0.25 μM and 0.25 μM as S/N = 3, respectively. The surface N-doping is an effective method to improve the electrochemical activity of GSEC film for AA sensing.

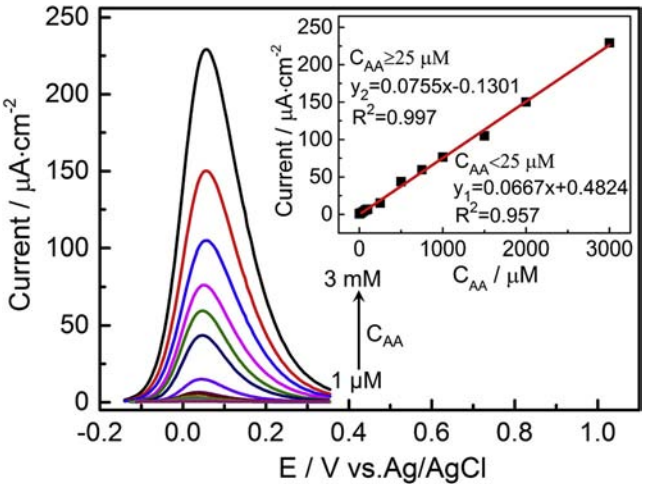

Fig. 7. DPVs of SN-GSEC film electrodes in 0.1 M PB solution (pH = 7.0) containing different concentrations of AA, from bottom to up, the concentrations from 1 μM to 3000 μM. The insert is the plot of the oxidation peak currents as a function of AA concentrations.

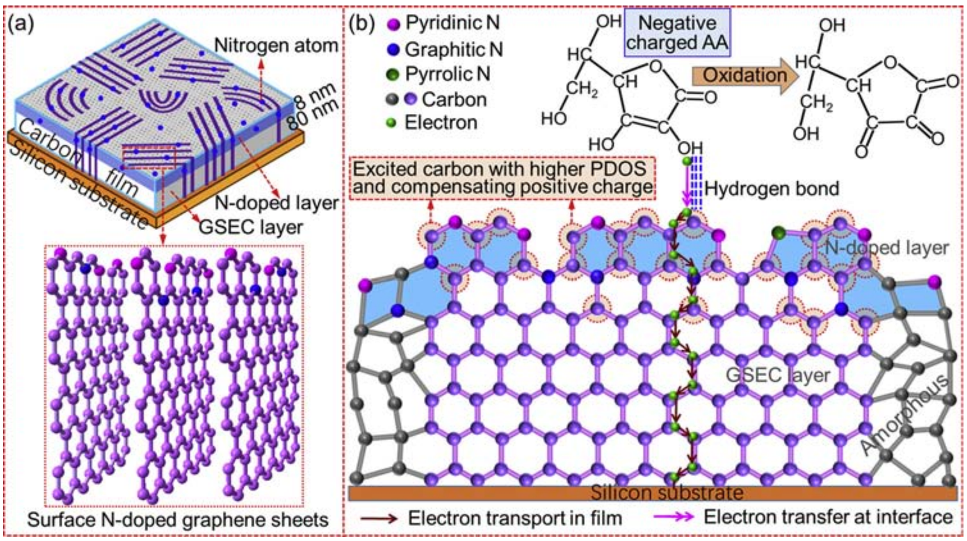

Fig. 6. (a) The microstructure diagram of SN-GSEC film: the under layer is the pure GSEC, the surface is N-doped. N-doped graphene sheets were formed and embedded in the amorphous carbon; (b) The mechanism diagram of surface N-doped graphene sheets electrocatalytic AA oxidation.

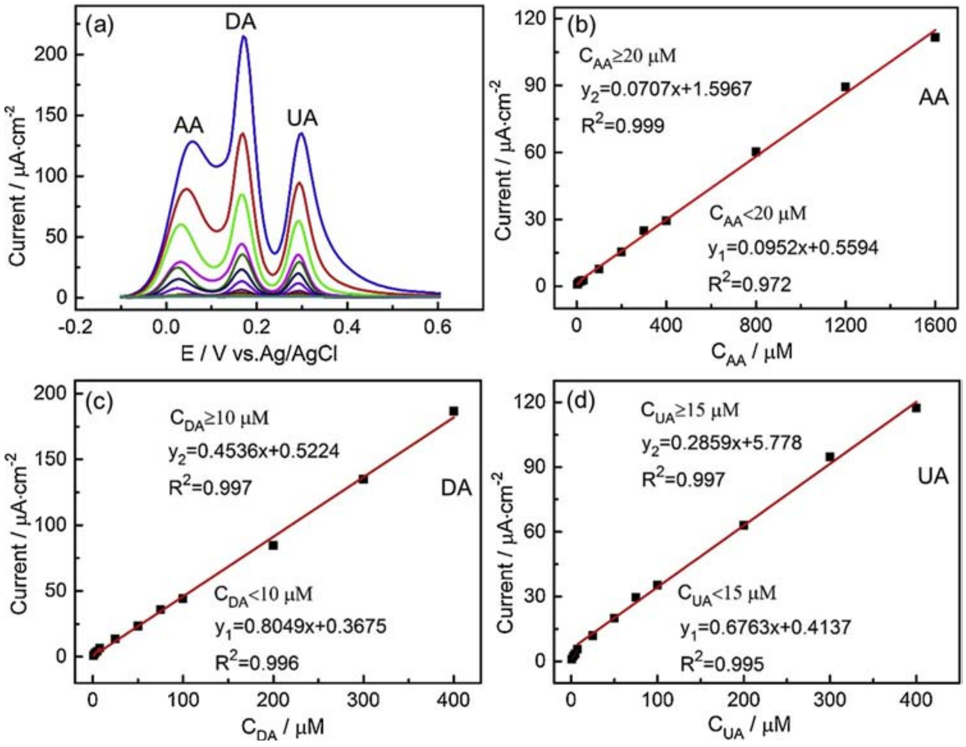

Fig. 8. (a) DPVs of SN-GSEC film electrodes in 0.1 M PB solution (pH = 7.0) containing different concentrations of AA, DA and UA. From bottom to up, the concentrations from 3 μM to 1600 μM for AA, 0.75 μM to 400 μM for DA and 0.75 μM to 400 μM for UA. (b)(c)(d) Plots of the oxidation peak currents as a function of AA, DA and UA concentrations, respectively.

Acknowledgements

This work was supported by the China Postdoctoral Science Foundation (grant numbers 2018M633124); National Nature Science Foundation of China (grant numbers 51575359), and Shenzhen Fundamental Research subject-layout project (grant numbers JCYJ20160427105015701). The authors are also grateful to the Electron Microscopy Center of Shenzhen University for helping in characterization of carbon film nanostructures.

Appendix A. Supplementary data

Supplementary material related to this article can be found, in the online version, at doi:https://doi.org/10.1016/j.snb.2018.12.079.

References

[1] Y. Yang, A. Jo, Y. Lee, C. Lee, Electrodeposited nanoporous ruthenium oxide for simultaneous quantification of ascorbic acid and uric acid using chronoamperometry at two different potentials, Sens. Actuators B Chem. 255 (2018) 316–324.

[2] F. Wantz, C.E. Banks, R.G. Compton, Direct oxidation of ascorbic acid at an edge plane pyrolytic graphite electrode: a comparison of the electroanalytical response with other carbon electrodes, Electroanalysis 17 (2005) 1529–1533.

[3] O. Arrigoni, M.C. De Tullio, Ascorbic acid: much more than just an antioxidant, Biochimica et Biophysica Acta (BBA) – Gen. Subj. 1569 (2002) 1–9.

[4] R.M. Wightman, C. Amatorh, R.C. Engstrom, P.D. Hale, E.W. Kristensen, W.G. Kuhr, L.J. May, Real-time characterization of dopamine overflow and uptake in the rat striatum, Neuroscience 25 (1988) 513–523.

[5] V.V.S.E. Dutt, H.A. Mottola, Determination of uric acid at the microgram level by a kinetic procedure based on a pseudo-induction period, Anal. Chem. 46 (1974) 1777–1781.

[6] M. Noroozifar, M. Khorasani-Motlagh, R. Akbari, M. Bemanadi Parizi, Simultaneous and sensitive determination of a quaternary mixture of AA, DA, UA and Trp using a modified GCE by iron ion-doped natrolite zeolite-multiwall carbon nanotube, Biosens. Bioelectron. 28 (2011) 56–63.

[7] S. Thiagarajan, S.-M. Chen, Preparation and characterization of PtAu hybrid film modified electrodes and their use in simultaneous determination of dopamine, ascorbic acid and uric acid, Talanta 74 (2007) 212–222.

[8] F. Valentini, A. Amine, S. Orlanducci, M.L. Terranova, G. Palleschi, Carbon nanotube purification: preparation and characterization of carbon nanotube paste electrodes, Anal. Chem. 75 (2003) 5413–5421.

[9] T.Y. You, O. Niwa, M. Tomita, T. Ichino, S. Hirono, Electrochemical oxidation of alkylphenols on ECR-sputtered carbon film electrodes with flat sub-nanometer surfaces, J. Electrochem. Soc. 149 (2002) E479–E484.

[10] O. Niwa, J. Jia, Y. Sato, D. Kato, R. Kurita, K. Maruyama, K. Suzuki, S. Hirono, Electrochemical performance of angstrom level flat sputtered carbon film consisting of sp2 and sp3 mixed bonds, J. Am. Chem. Soc. 128 (2006) 7144–7145.

[11] N. Sekioka, D. Kato, A. Ueda, T. Kamata, R. Kurita, S. Umemura, S. Hirono, O. Niwa, Controllable electrode activities of nano-carbon films while maintaining surface flatness by electrochemical pretreatment, Carbon 46 (2008) 1918–1926.

[12] A. Ueda, D. Kato, N. Sekioka, T. Kamata, R. Kurita, H. Uetsuka, Y. Hattori, S. Hirono, S. Umemura, O. Niwa, Fabrication of electrochemically stable fluorinated nano-carbon film compared with other fluorinated carbon materials, Carbon 47 (2009) 1943–1952.

[13] C. Wang, X. Zhang, D.F. Diao, Nanosized graphene crystallite induced strong magnetism in pure carbon films, Nanoscale 7 (2015) 4475–4481.

[14] L. Huang, Y. Cao, D. Diao, Nanosized graphene sheets induced high electrochemical activity in pure carbon film, Electrochim. Acta 262 (2018) 173–181.

[15] J.-B. Raoof, R. Ojani, A. Kiani, Carbon paste electrode spiked with ferrocene carboxylic acid and its application to the electrocatalytic determination of ascorbic acid, J. Electroanal. Chem. 515 (2001) 45–51.

[16] J. Huang, Y. Liu, H. Hou, T. You, Simultaneous electrochemical determination of dopamine, uric acid and ascorbic acid using palladium nanoparticle-loaded carbon nanofibers modified electrode, Biosens. Bioelectron. 24 (2008) 632–637.

[17] Y.-R. Kim, S. Bong, Y.-J. Kang, Y. Yang, R.K. Mahajan, J.S. Kim, H. Kim, Electrochemical detection of dopamine in the presence of ascorbic acid using graphene modified electrodes, Biosens. Bioelectron. 25 (2010) 2366–2369.

[18] Y. Qi, H. Long, L. Ma, Q. Wei, S. Li, Z. Yu, J. Hu, P. Liu, Y. Wang, L. Meng, Enhanced selectivity of boron doped diamond electrodes for the detection of dopamine and ascorbic acid by increasing the film thickness, Appl. Surf. Sci. 390 (2016) 882–889.

[19] C. Ueda, D.C.-S. Tse, T. Kuwana, Stability of catechol modified carbon electrodes for electrocatalysis of dihydronicotinamide adenine dinucleotide and ascorbic acid, Anal. Chem. 54 (1982) 850–856.

[20] L. Zhang, X. Lin, Covalent modification of glassy carbon electrode with glutamic acid for simultaneous determination of uric acid and ascorbic acid, Analyst 126 (2001) 367–370.

[21] Z.-H. Sheng, X.-Q. Zheng, J.-Y. Xu, W.-J. Bao, F.-B. Wang, X.-H. Xia, Electrochemical sensor based on nitrogen doped graphene: simultaneous determination of ascorbic acid, dopamine and uric acid, Biosens. Bioelectron. 34 (2012) 125–131.

[22] T. Kamata, D. Kato, S. Hirono, O. Niwa, Structure and electrochemical performance of nitrogen-doped carbon film formed by electron cyclotron resonance sputtering, Anal. Chem. 85 (2013) 9845–9851.

[23] M.F. John, S.F. William, S.E. Peter, B.D. Kenneth, Handbook of X-ray Photoelectron Spectroscopy, Physical Electronics, Inc., Minnesota, 1995.

[24] R.J.J. Jansen, H. van Bekkum, XPS of nitrogen-containing functional groups on activated carbon, Carbon 33 (1995) 1021–1027.

[25] A.C. Ferrari, J. Robertson, Interpretation of Raman spectra of disordered and amorphous carbon, Phys. Rev. B 61 (2000) 14095–14107.

[26] D. Graf, F. Molitor, K. Ensslin, C. Stampfer, A. Jungen, C. Hierold, L. Wirtz, Spatially resolved Raman spectroscopy of single- and few-layer graphene, Nano Lett. 7

(2007) 238–242.

[27] D. Wei, Y. Liu, Y. Wang, H. Zhang, L. Huang, G. Yu, Synthesis of N-doped graphene by chemical vapor deposition and its electrical properties, Nano Lett. 9 (2009) 1752–1758.

[28] D. Guo, R. Shibuya, C. Akiba, S. Saji, T. Kondo, J. Nakamura, Active sites of nitrogen-doped carbon materials for oxygen reduction reaction clarified using model catalysts, Science 351 (2016) 361–365.

[29] J. Li, Y. Zhang, X. Zhang, J. Huang, J. Han, Z. Zhang, X. Han, P. Xu, B. Song, S, N Dual-Doped Graphene-like Carbon Nanosheets as Efficient Oxygen Reduction Reaction Electrocatalysts, ACS Appl. Mater. Interfaces 9 (2017) 398–405.

[30] H.-B. Wang, H.-D. Zhang, S.-P. Xu, T. Gan, K.-J. Huang, Y.-M. Liu, A sensitive and label-free electrochemical impedance biosensor for protein detection based on terminal protection of small molecule-linked DNA, Sens. Actuators B Chem. 194 (2014) 478–483.

[31] L. Hu, X. Peng, K. Huo, R. Chen, J. Fu, Y. Li, L.Y.S. Lee, K.-Y. Wong, P.K. Chu, Dominant factors governing the electron transfer kinetics and electrochemical biosensing properties of carbon nanofiber arrays, ACS Appl. Mater. Interfaces 8 (2016) 28872–28879.

[32] E. Luais, M. Boujtita, A. Gohier, A. Tailleur, S. Casimirius, M.A. Djouadi, A. Granier, P.Y. Tessier, Carbon nanowalls as material for electrochemical transducers, Appl. Phys. Lett. 95 (2009) 3049.

[33] X. Yang, L. Haubold, G. DeVivo, G.M. Swain, Electroanalytical performance of nitrogen-containing tetrahedral amorphous carbon thin-film electrodes, Anal. Chem. 84 (2012) 6240–6248.

[34] N.W. Khun, E. Liu, H.W. Guo, Cyclic voltammetric behavior of nitrogen-doped tetrahedral amorphous carbon films deposited by filtered cathodic vacuum arc, Electroanalysis 20 (2008) 1851–1856.

[35] D. Liu, X. Zhang, T. You, Electrochemical performance of electrospun free-standing nitrogen-doped carbon nanofibers and their application for glucose biosensing, ACS Appl. Mater. Interfaces 6 (2014) 6275–6280.

[36] A. Ambrosi, A. Bonanni, M. Pumera, Electrochemistry of folded graphene edges, Nanoscale 3 (2011) 2256–2260.

[37] K. Siuzdak, M. Ficek, M. Sobaszek, J. Ryl, M. Gnyba, P. Niedziałkowski, N. Malinowska, J. Karczewski, R. Bogdanowicz, Boron-enhanced growth of micron-scale carbon-based nanowalls: a route toward high rates of electrochemical biosensing, ACS Appl. Mater. Interfaces 9 (2017) 12982–12992.

[38] A.J. Bard, L.R. Faulkner, Electrochemical Methods: Fundamental and Applications, 2nd ed, John Wiley and Sons, New York, 2001.

[39] G. Yongjun, H. Gang, Z. Jun, S. Zujin, Z. Yuanshuai, S.D. Sheng, W. Jianguo, B. Xinhe, M. Ding, Nitrogen-doped sp2-hybridized carbon as a superior catalyst for selective oxidation, Angew. Chem. Int. Ed. 52 (2013) 2109–2113.

[40] W. Yin, T.-T. Jia, X. Guo, X. Huang, Y.-F. Zhang, W.-K. Chen, Effects of N-doping concentration on graphene structures and properties, Chem. Phys. Lett. 581 (2013) 74–79.

[41] J. Lahaye, G. Nansé, A. Bagreev, V. Strelko, Porous structure and surface chemistry of nitrogen containing carbons from polymers, Carbon 37 (1999) 585–590.

[42] P. Hirunsit, M. Liangruksa, P. Khanchaitit, Electronic structures and quantum capacitance of monolayer and multilayer graphenes influenced by Al, B, N and P doping, and monovacancy: theoretical study, Carbon 108 (2016) 7–20.

[43] A. Omidvar, Electronic structure tuning and band gap opening of nitrogen and boron doped holey graphene flake: the role of single/dual doping, Mater. Chem. Phys. 202 (2017) 258–265.

[44] A.M. Pisoschi, A. Pop, A.I. Serban, C. Fafaneata, Electrochemical methods for ascorbic acid determination, Electrochim. Acta 121 (2014) 443–460.

[45] T. Palomäki, N. Wester, L.-S. Johansson, M. Laitinen, H. Jiang, K. Arstila, T. Sajavaara, J.G. Han, J. Koskinen, T. Laurila, Characterization and electrochemical properties of oxygenated amorphous carbon (a-c) films, Electrochim. Acta 220 (2016) 137–145.

[46] H. Zhang, Q. Huang, Y. Huang, F. Li, W. Zhang, C. Wei, J. Chen, P. Dai, L. Huang, Z. Huang, L. Kang, S. Hu, A. Hao, Graphitic carbon nitride nanosheets doped graphene oxide for electrochemical simultaneous determination of ascorbic acid, dopamine and uric acid, Electrochim. Acta 142 (2014) 125–131.

[47] A.M. Oliveira-Brett, L.Ad. Silva, C.M.A. Brett, Adsorption of guanine, guanosine, and adenine at electrodes studied by differential pulse voltammetry and electrochemical impedance, Langmuir 18 (2002) 2326–2330.

[48] C.M.A. Brett, A.M.O. Brett, Electrochemistry: Principles, Methods, and Applications, Oxford Press, 1993.

[49] H. Dongxue, H. Tingting, S. Changsheng, I. Ari, N. Li, Simultaneous determination of ascorbic acid, dopamine and uric acid with chitosan-graphene modified electrode, Electroanalysis 22 (2010) 2001–2008.